Molecular Crystals and Liquid Crystals
Publication details, including instructions for authors and subscription information:
http://www.tandfonline.com/loi/gmcl20

Synthesis, Crystal Structure, and Spectroscopic and Electronic Properties of N-[4-(3-Methyl-3-Phenyl-Cyclobutyl)-Thiazol-2-yl]-N′-Phenyl Hydrazine

H. Saraçoğlu [a], F. Güntepe [b], Ç. Yüksektepe [c], N. Çalişkan [b] & A. Cukurovali [d]

[a] Department of Middle Education, Educational Faculty, Ondokuz Mayis University, 55139, Kurupelit, Samsun, Turkey

[b] Department of Physics, Faculty of Arts and Sciences, Ondokuz Mayis University, 55139, Kurupelit, Samsun, Turkey

[c] Department of Physics, Faculty of Science, Çankırı Karatekin University, 18100, Ballıca, Çankırı, Turkey

[d] Department of Chemistry, Faculty of Science, Firat University, 23119, Elazig, Turkey

Version of record first published: 07 Oct 2011

To cite this article: H. Saraçoğlu, F. Güntepe, Ç. Yüksektepe, N. Çalişkan & A. Cukurovali (2011): Synthesis, Crystal Structure, and Spectroscopic and Electronic Properties of N-[4-(3-Methyl-3-Phenyl-Cyclobutyl)-Thiazol-2-yl]-N′-Phenyl Hydrazine, Molecular Crystals and Liquid Crystals, 548:1, 237-255

To link to this article: http://dx.doi.org/10.1080/15421406.2011.590334

Mol. Cryst. Liq. Cryst., Vol. 548: pp. 237–255, 2011

ISSN: 1542-1406 print/1563-5287 online
DOI: 10.1080/15421406.2011.590334

Taylor & Francis
Taylor & Francis Group

Synthesis, Crystal Structure, and Spectroscopic and Electronic Properties of *N*-[4-(3-Methyl-3-Phenyl-Cyclobutyl)-Thiazol-2-yl]-*N′*-Phenyl Hydrazine

H. SARAÇOĞLU,[1,*] F. GÜNTEPE,[2] Ç. YÜKSEKTEPE,[3] N. ÇALIŞKAN,[2] AND A. CUKUROVALI[4]

[1]Department of Middle Education, Educational Faculty, Ondokuz Mayis University, 55139 Kurupelit, Samsun, Turkey
[2]Department of Physics, Faculty of Arts and Sciences, Ondokuz Mayis University, 55139 Kurupelit, Samsun, Turkey
[3]Department of Physics, Faculty of Science, Çankırı Karatekin University, 18100 Ballıca, Çankırı, Turkey
[4]Department of Chemistry, Faculty of Science, Firat University, 23119 Elazig, Turkey

The title molecule, N-[4-(3-Methyl-3-phenyl-cyclobutyl)-thiazol-2-yl]-N′-phenyl hydrazine ($C_{20}H_{21}N_3S$), was prepared and characterized by elemental analysis, ^{1}H-NMR, ^{13}C-NMR, FT-IR, UV-Visible (UV-Vis), and single-crystal X-ray diffraction. The compound crystallizes in the monoclinic space group $P2_1/c$ with $a = 12.2960(5)$, $b = 13.9565(5)$, $c = 10.6356(5)$ Å, and $\beta = 99.106(3)^\circ$. Molecular geometries from X-ray experiment, vibrational frequencies, atomic charges distribution, dipole moments and total energies of the title compound and the dimer in the ground state have been calculated using the density functional theory method (RB3LYP) with 6-31G(d, p) and 6-311G(d, p) basis sets, and compared with the experimental data. Calculated results show that DFT at the RB3LYP/6-31G(d, p) and 6-311G(d, p) levels can well reproduce the structure of the title compound. To determine conformational flexibility, the molecular energy profile of the title compound was obtained by semi-empirical (RAM1) calculations with respect to the selected torsion angle, which was varied from -180° to $+180^\circ$ in steps of 10°. In addition, the molecular electrostatic potential (MEP), frontier molecular orbitals, thermodynamic properties, and UV-Vis absorption spectra of the title compound were investigated using theoretical calculations. UV-Vis absorption spectra of the compound have been ascribed to their corresponding molecular structure and electrons orbital transitions.

Keywords DFT calculations; hydrazine derivative; IR spectra; X-ray structure determination

*Address correspondence to Hanife Saraçoğlu, Department of Middle Education, Educational Faculty, Ondokuz Mayis University, TR-55139, Kurupelit, Samsun, Turkey. Fax: +90-362-4576078. E-mail: hanifesa@omu.edu.tr

1. Introduction

Hydrazine is a highly reactive molecule used as a rocket propellant and an antioxidant in water systems, and is used to produce plastic blowing agents. It is also a minor metabolite of two important drugs, namely isoniazid, an antitubercular agent, and hydralazine, an antihypertensive agent [1,2]. It has been said that hydrazine causes depletion of ATP and GSH (glutathione) and the accumulation of triglycerides in the liver [3] as well as neurological effects in experimental rats [4]. It is also a putative carcinogen [5]. The mechanisms of hydrazine toxicity are not fully understood, although the accumulation of triglycerides is in part due to the increased mobilization of fats from adipose tissues coupled with a reduction in the transport of triglycerides out of the liver [6,7]. Hydrazine has been reported to methylate DNA [8] and interfere in the urea cycle, with the result that citrulline levels are raised in the livers of experimental animals [9,10]. Substituted hydrazines have also found many scientific and commercial applications [11,12]. Thiazole itself and its derivatives are of importance in biological systems as anti-inflammatory, analgesic agents and inhibitors of lipoxygenase activities [13,14]. On the other hand, cyclobutane amino acids in different structures were described as highly potent l-glutamate, N-methyl-D-aspartate (NMDA) agonists, NMDA antagonists, and anticonvulsive drugs [15–17].

In recent years, density functional theory (DFT) has been a shooting star in theoretical modeling. The development of ever better exchange-correlation functionals has made it possible to calculate many molecular properties with accuracies comparable to those of traditional correlated ab initio methods, with more favorable computational costs [18]. Literature surveys have revealed the high degree of accuracy of DFT methods in reproducing the experimental values in terms of geometry, dipole moment, vibrational frequency, etc. [19–25].

In the present paper, we report the synthesis, and structural and spectral characterizations of *N*-[4-(3-Methyl-3-phenyl-cyclobutyl)-thiazol-2-yl]-*N'*-phenyl hydrazine together with DFT computational studies. The structural geometry, electronic charge distribution, molecular electrostatic potential (MEP), and thermodynamic properties of the title compound at the B3LYP/6-31G(d, p) level were studied. In addition, experimental and theoretical results were compared.

2. Experiment

2.1. Synthesis of the Title Compound

Phenyl hydrazine and NH_4SCN were purchased from Merck and used as received. 1-methyl-1-phenyl-3-(2-chloro-1-oxoethyl) cyclobutane was synthesized according to the literature procedure [26]. The compound was synthesized as shown in Scheme 1. To a stirred solution of phenyl hydrazine (10 mmol) in 30 mL of ethanol, ammonium rhodanide (10 mmol) in 20 mL of water was added. Subsequently, a solution of 1-methyl-1-phenyl-3-(2-chloro-1-oxoethyl) cyclobutane (α-haloketone) (10 mmol) in ethanol (20 mL) was added dropwise. After the addition of α-haloketone, the temperature was kept at 323–328 K for more than 2 h. After cooling to room temperature, the solution was then made alkaline with an aqueous solution of NH_3 (5%), and a light orange precipitate separated. The precipitate was filtered off, washed with aqueous NH_3 solution several times, and dried in air. Suitable single crystals for crystal structure determination were obtained by slow evaporation of its ethanol solution [yield: 84%, melting point: 464 K. Characteristic

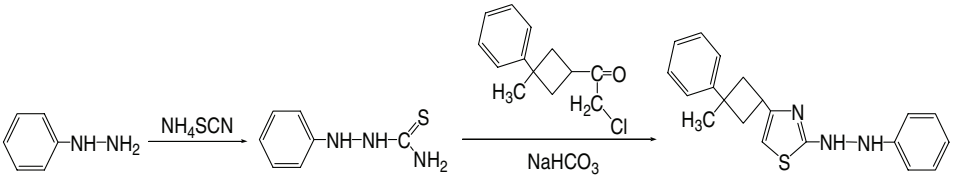

Scheme 1. Synthetic route for the synthesis of the target compound.

^{1}H-NMR shifts (DMSO-d_6, δ, ppm): 1.51 (s, 3H, $-CH_3$ in cyclobutane), 2.33–2.38 (m, 2H, $-CH_2-$ in cyclobutane), 2.47–2.52 (m, 2H, $-CH_2-$ in cyclobutane), 3.54 (q, $j = 8.78$ Hz, 1H, $>C-H$ in cyclobutane), 6.28 (s, 1H, $= CH-S$), 6.70–6.75 (m, 3H, aromatics), 7.11–7.16 (m, 5H, aromatics), 7.28–7.31 (m, 2H, aromatics), 8.18 (s 1H, $-NH-$ D_2O exchangeable), 9.28 (s, 1H, $-NH-$ D_2O exchangeable). Characteristic ^{13}C-NMR shifts (DMSO-d_6, δ, ppm): 175.31, 157.10, 153.04, 149.23, 129.56, 128.85, 125.87, 125.27, 119.81, 112.91, 101.24, 40.79, 38.91, 31.29, 30.73. Elemental analysis for $C_{20}H_{21}N_3S$ (335.47 gmol^{-1}): Calculated: C: 71.61; H: 6.31; N: 12.53; S: 9.56. Found. C: 71.44; H: 6.37; N: 12.71; S: 9.88].

2.2. Measurement

IR spectrum was recorded on an ATI Unicam-Mattson 1000 FT-IR spectrometer using KBr pellets. ^{1}H-NMR and ^{13}C-NMR spectra were obtained using a Bruker 300 MHz spectrometer. The UV spectrum of the compound was performed on a Shimadzu UV-1700 spectrometer in a $CHCl_3$ solvent.

2.3. X-Ray Crystallography

The data collection was performed at 296 K on a Stoe-IPDS-2 diffractometer equipped with a graphite monochromated Mo-K_α radiation ($\lambda = 0.71073$ Å). The structure was solved by direct methods using SHELXS-97 and refined by a full-matrix least-squares procedure using the program *SHELXL-97* [27]. All non-hydrogen atoms were easily found from the difference Fourier map and refined anisotropically. All hydrogen atoms of carbons and nitrogens were included using a riding model and refined isotropically with CH = 0.93 (for phenyl groups), $CH_2 = 0.97$, $CH_3 = 0.96$, CH = 0.98, and NH = 0.86 Å [$U_{iso}(H) = 1.2U_{eq}$ (1.5 U_{eq} for methyl group)]. Details of the data collection conditions and the parameters of the refinement process are given in Table 1.

3. DFT Calculations

The geometric optimization of the compound in the ground state (in vacuo) was performed on a personal computer using experimental geometry as input, employing the *GAUSSIAN-03* program at DFT with the RB3LYP/6-31G(d, p) and RB3LYP/6-311G(d, p) levels [28]. Furthermore, the geometry of two molecules linked by N—H... N hydrogen bonding was taken from the experimental X-ray data and a full-geometry optimization on the molecules, named as a dimer was carried out with the RB3LYP/6-31G(d, p) level. Then,

Table 1. Crystallographic data of the title compound

Empirical formula	$C_{20}H_{21}N_3S_1$
M_r	335.46
T (K)	296
Radiation, λ (Å)	0.71073
Crystal system	Monoclinic
Space group	$P2_1/c$
Unit cell dimensions	
a (Å)	12.2960(5)
b (Å)	13.9565(5)
c (Å)	10.6356(5)
β (Å)	99.106(3)
V (Å^3)	1802.16(13)
Z	4
D_c (g cm^{-3})	1.236
μ/mm^{-1}	0.185
F(000)	712
Crystal size (mm)	0.620 × 0.423 × 0.080
Θ range (°)	1.7/27.5
Index range (h, k, l)	−15/15, −18/18, −13/13
Reflections collected	27035
Independent reflections (R_{int})	4132 (0.035)
Observed reflections[$I > 2\sigma(I)$]	3123
T_{min}, T_{max}	0.8392, 0.9332
Data/parameters	4132/218
Goodness of fit on F^2	1.03
Final R indices [$I > 2\sigma(I)$]	0.035
wR indices [$I > 2\sigma(I)$]	0.089
Largest diff. peak and hole (e. Å^{-3})	0.29 and −0.31

we calculated vibrational frequencies for optimized molecular structures and scaled them by 0.9806. To identify low-energy conformation, the selected degree of torsion angle, T(C2−C3−C5−C10), was varied from −180° to +180° in steps of 10°, and the molecular energy profile was obtained at the semi-empirical RAM1 level.

The MEP was evaluated to research the reactive sites of the title compound using the B3LYP/6-31G(d, p) level. On the basis of vibrational analysis, the thermodynamic properties of the molecule at different temperatures were calculated. In addition, frontier molecular orbital (FMO) analysis was carried out with the same level.

4. Results and Discussion

4.1. Description of the Crystal Structure

The title compound, an ORTEP-3 view of which is shown in Fig. 1, crystallizes in the monoclinic space group $P2_1/c$ with four molecules in the unit cell [29]. The asymmetric unit in the crystal structure contains only one molecule.

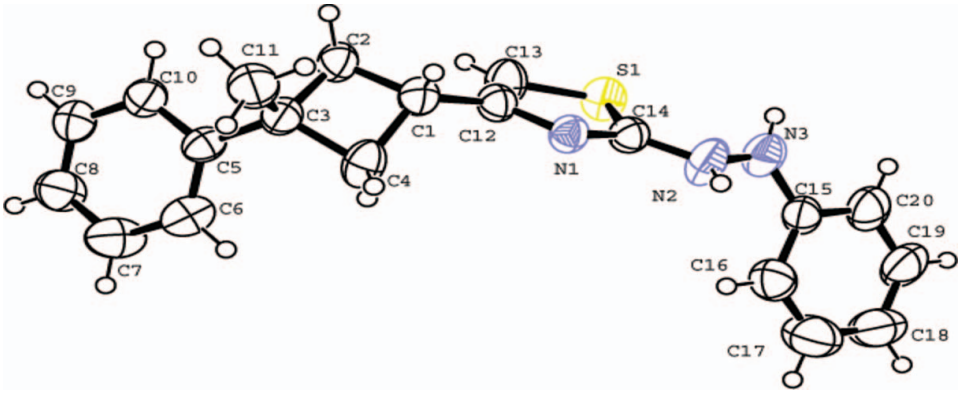

Figure 1. ORTEP drawing of the basic crystallographic unit, showing the atom numbering scheme. Displacement ellipsoids are drawn at the 30% probability level and H atoms are shown as small spheres of arbitrary radii.

The title molecule is composed of a central thiazole ring, with a phenyl hydrazine group connected to the 2-position of the ring and a (3-methyl-3-phenyl)cyclobutyl group in the 4-position. The cyclobutane ring A (C1-C4), the thiazole ring B (S1/C14/N1/C12/C13), the phenyl ring C (C5-C10), and the other phenyl ring D (C15-C20) are planar. The dihedral angles between these planes are 46.95(9)°, 36.64(10)°, 37.78(11)°, 80.17 (6)°, 64.16 (6)°, and 58.06 (6)° for A/B, A/C, A/D, B/C, B/D, and C/D, respectively. In the thiazole ring, the S1—C13 and S1—C14 bond lengths (Table 3) are shorter than the accepted value for an S—Csp^2 single bond with 1.76 Å, resulting from the conjugation of the electrons of the S1 with atoms C13 and C14 [30].

In the cyclobutane ring A, the C4/C1/C2 plane forms a dihedral angle of 29.80 (20)° with the C2/C3/C4 plane. This value is significantly greater than those in the literatures: 23.5° [31], 18.92(15)° [32], and 19.26(17)° [33]. The geometry of the cyclobutane ring is due to the steric effect of the methyl group.

The thiazole ring and the phenyl ring D are linked by a hydrazine group with −126.90(18)° torsion angle. The molecules are linked in a head-to-head fashion by N—H . . . N hydrogen bonding (Table 2). In this hydrogen bonding, the atom N2 at (*x*, *y*, *z*) acts as a donor to atom N1 at (–*x*, 1 – *y*, 1 – *z*). As a result, these interactions formed a hydrogen-bonded dimer of graph set motif $R_2^2(8)$ ring at (*m*, *n* + 1/2, *k* + 1/2) (the other ring is formed between the molecule with symmetry

Table 2. Hydrogen bonds geometries of the crystal structure (Å, °)

D—H . . . A	D—H	H . . . A	D . . . A	D—H . . . A
N2—H2 . . . $N1^{i}$	0.86	2.14	2.975(2)	163
C13—H13 . . . $Cg3^{ii}$	0.93	2.70	3.409(2)	134
C11—H11B . . . $Cg4^{i}$	0.96	2.91	3.768(3)	149

Notes. Cg3 is the centroid of the C ring; Cg4 is the centroid of the D ring. Symmetry code: (i) −*x*, 1 – *y*, 1 – *z*; (ii): *x*, 1/2 – *y*, 1/2 + *z*.

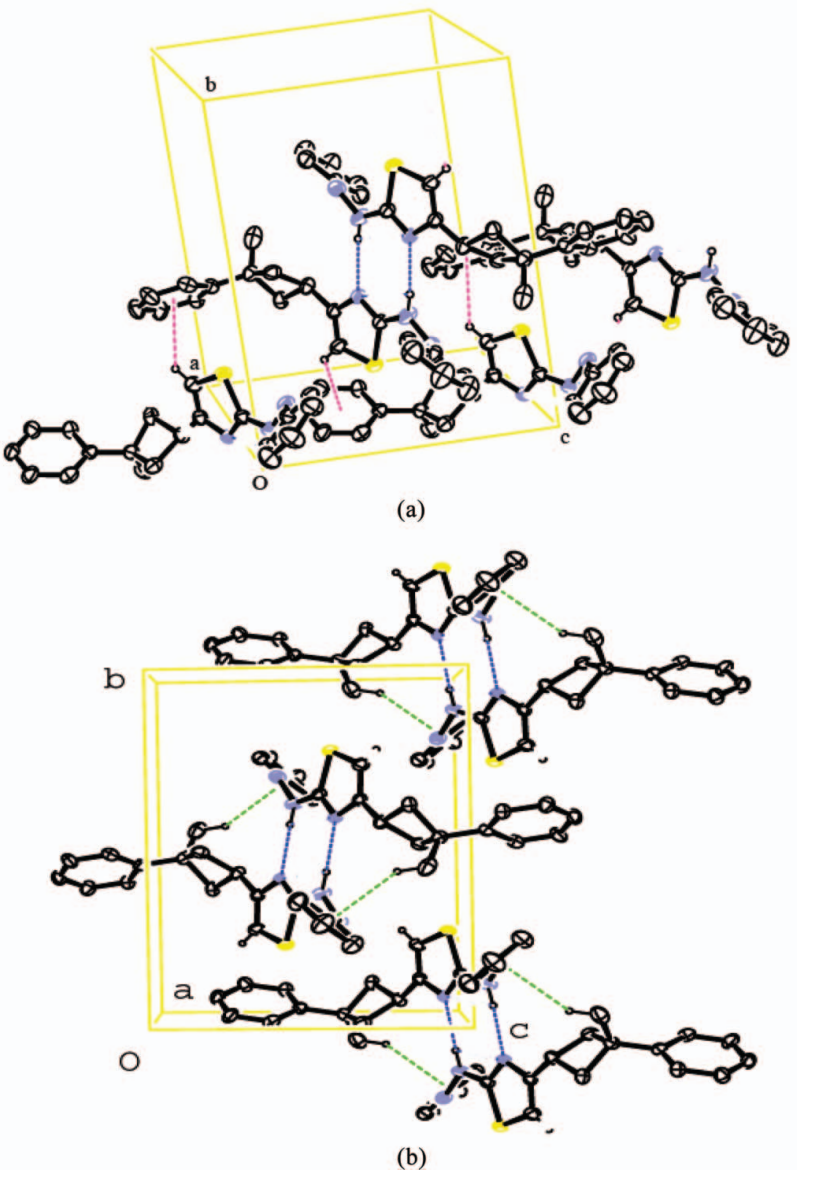

Figure 2. (a) Diagram showing the hydrogen bond and π-ring interactions in the title compound. Only those H atoms involved in the hydrogen bonding interactions are shown (symmetry codes: $-x$, $1 - y$, $1 - z$ and x, $1/2 - y$, $1/2 + z$). (b) Partial packing diagram for the compound, showing the N—H... N and C—H... π interactions as broken lines. Hydrogen atoms not involved in hydrogen bonding have been omitted (symmetry code: $-x$, $1 - y$, $1 - z$).

code ($-x$, $y - 1/2$, $1/2 - z$) and the molecule with symmetry code (x, $1/2 - y$, $z - 1/2$) by same N—H... N hydrogen bonding [34]. Also as a result, these interactions formed a hydrogen-bonded dimer of graph set motif $R_2^2(8)$ ring at (m, n, k), (where m, n, and k are integers). These dimers are linked by C—H... π intermolecular

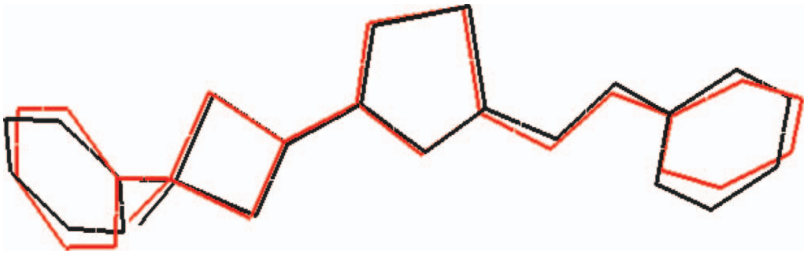

Figure 3. Comparison of the molecular conformation of the compound as established from X-ray study (black line) and solid-state DFT calculation with 6-31G(d, p) basis set (red line). Hydrogen atoms have been omitted for clarity.

hydrogen bonds, as shown Fig. 2(b). The other C—H$\ldots\pi$ intermolecular hydrogen bonds are also effective in the crystal packing, as shown in Fig. 2(a) and Table 2[1].

4.2. Optimized Structure

DFT calculations were performed on the title compound at the RB3LYP/6-31G(d, p) and RB3LYP/6-311G(d, p) levels. Some optimized geometric parameters are also listed in Table 3. Comparing the theoretical values with the experimental ones indicates that all of the optimized bond lengths are slightly larger than the experimental values, as the theoretical calculations are performed for an isolated molecule in gaseous phase and the experimental results are for a molecule in solid state. Thus, it was also compared with a dimeric structure of the title compound using the DFT RB3LYP method with 6-31G(d, p) basis set. As a result, using the root mean square error (RMSE) for evaluation, the dimeric structure best predicts the bond distances, with an error of 0.016 Å, whereas the monomeric structure best predicts the bond angles, with an error of 0.466°.

The dihedral angles between optimized counterparts of the title compound are calculated at 45.57° (A/B), 36.61° (A/C), 41.84° (A/D), 75.09° (B/C), 74.29° (B/D), and 59.25° (C/D) for 6-31G(d, p), and at 30.91° (A/B), 45.08° (A/C), 68.49° (A/D), 75.21° (B/C), 74.29° (B/D), and 60.46° (C/D) for 6-311G(d, p). For the cyclobutane ring, the dihedral angle between the C4/C1/C2 and the C2/C3/C4 plane is 29.80 (20)°, whereas the dihedral angle has been calculated at 7.35° for 6-31G(d, p), and at 24.58° for 6-311G(d, p).

4.3. Conformational Analysis

The X-ray structure of the title compound is compared with its DFT-optimized counterpart (see Fig. 3), where conformational differences are shown between them. These differences are given as RMSE of 0.402 Å for the RB3LYP/6-31G(d, p) level, and 0.385 Å for the RB3LYP/6-311G(d, p) level. The calculated energy profile from RAM1 versus the torsion angle C2—C3—C5—C10 is given in Fig. 4. The respective value of the selected degree of torsion angle, T(C2—C3—C5—C10), is −54.2(2)° in the X-ray structure, whereas the corresponding value in the optimized geometry is −41.2067° for B3LYP/6-31G(d, p),

[1]Crystallographic data for the structural analysis have been deposited with the Cambridge Crystallographic Data Centre, CCDC No 735319. Copies of this information may be obtained free of charge from the Director, CCDC, 12 Union Road, Cambridge CB2 1EZ, United Kingdom (fax: +44-1223-336033; E-mail: deposit@ccdc.cam.ac.uk; Website: www: http://www.ccdc.cam.ac.uk)

Table 3. Selected theoretical and experimental geometric parameters for the title compound (bond lengths in Å, bond angles in degrees)

		DFT (monomer)		DFT (dimer)
	Experimental	6-31G(d, p)	6-311G(d, p)	6-31G(d, p)
Bond length (Å)				
S1−C13	1.732(2)	1.7522	1.7521	1.7536
S1−C14	1.7304(16)	1.7612	1.7586	1.7624
N1−C12	1.3848(19)	1.3905	1.3879	1.3935
N1−C14	1.306(2)	1.2989	1.2950	1.3098
N2−C14	1.350(2)	1.3825	1.3813	1.3650
N2−N3	1.393(2)	1.3900	1.3880	1.3898
C3−C5	1.508(2)	1.5174	1.5161	1.5178
C3−C11	1.531(3)	1.5397	1.5387	1.5393
RMSE[a]		0.018	0.018	0.016
Max. difference[a]		0.032	0.031	0.032
Bond angle (°)				
C13−S1−C14	87.84(8)	87.4204	87.4280	87.8792
C14−N2−N3	117.82(15)	117.4810	117.8078	117.0860
N2−N3−C15	116.94(15)	117.5519	117.8605	118.2124
C12−N1−C14	110.17(13)	110.4908	110.8051	111.0894
C5−C3−C11	109.11(15)	109.7759	109.7818	109.8481
C11−C3−C2	111.40(17)	111.7019	111.6337	111.7818
RMSE[a]		0.466	0.567	0.785
Max. difference[a]		0.666	0.920	1.272
Dihedral angles (°)				
S1−C14−N2−N3	3.6(2)	22.4445	21.4196	14.0326
N1−C14−N2−N3	−175.89(16)	−160.0475	−161.0163	−167.5148
N2−N3−C15−C16	15.5(3)	24.5944	23.2140	19.9697
N2−N3−C15−C20	−166.17(17)	−157.7997	−159.3262	−162.6540
C14−N2−N3−C15	−126.90(18)	−140.2193	−137.9965	−130.7930

[a]RMSE and maximum differences between the bond lengths and the bond angles were computed by the theoretical method and those obtained from X-ray diffraction.

−41.2709° for B3LYP /6-311G(d, p), and −40.6251° for the dimer. According to Fig. 4, the minimum energy is located at −40°, having energy of 126.447 kcal mol^{-1}, and the maximum energy is also located at 90°, having energy of 128.719 kcal mol^{-1}. The energy difference between the most favorable and the most unfavorable conformer, which arises from rotational potential barrier calculated with respect to the selected torsion angle, is calculated as 2.272 kcal mol^{-1} when both selected degrees of torsion angle are considered.

The molecular energy can be divided into bonded and non-bonded contributions. The bonded energy is considered to be independent of torsion angle changes and therefore vanished when relative conformer energies were calculated. The non-bonded energy is further separated into torsional steric and electrostatic terms. Hydrogen bond is an intense electrostatic contribution [35]. Since there is no intramolecular hydrogen bond in the title compound, the calculated structure is the most stable conformer, which is principally

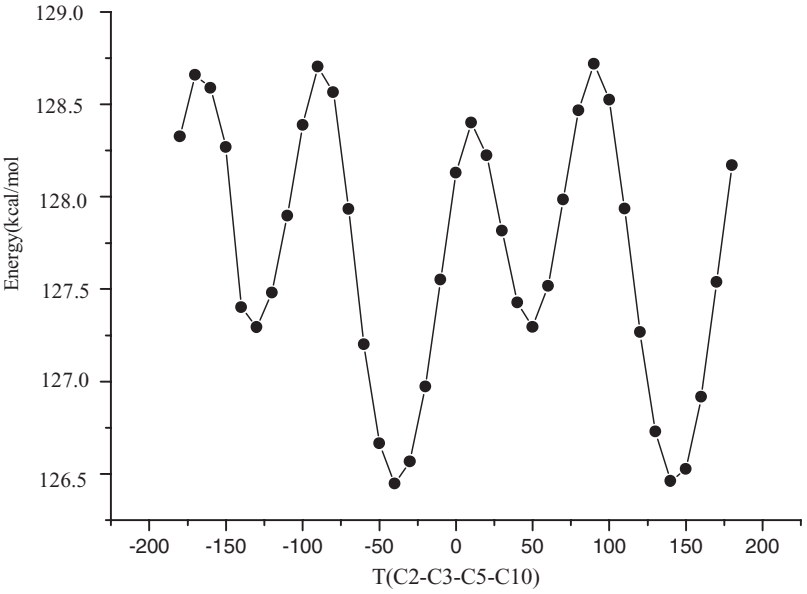

Figure 4. Molecular energy profile of the optimized counterpart of the title compound versus selected degrees of torsion angle.

determined by the non-bonded torsional energy and electrostatic energy terms affected by packing of the molecules.

4.4. Mulliken Atomic Charges and Molecular Electrostatic Potential

The Mulliken atomic charges were calculated at the RB3LYP/6-31G(d, p) and RB3LYP/6-311G(d, p) levels and are illustrated in Table 4. Atomic charge analysis revealed that the negative charges on the nitrogen and carbon atoms (C11, C13) are significantly greater than the other atoms, but the positive charges are expected to be localized on the protonated N2 atom and carbon (C11, C13) atoms. However, the calculations show that the positive charges on hydrogen atoms bound to the N2, C11, and C13 atoms are found to be greater than those on other hydrogen atoms in the title compound. Thus, the positive charges may be delocalized between N2, C11, C13, and hydrogen atoms.

The molecular electrostatic potential, $V(r)$, at a given point $r(x, y, z)$ in the vicinity of a molecule, is defined in terms of the interaction energy between the electrical charge generated from the molecule's electrons and nuclei and a positive test charge (a proton) located at r. For the system studied, the $V(r)$ values were calculated as described previously using the following equation [36]:

$$V(r) = \Sigma Z_A/|R_A - r| - \int \rho(r')/|r' - r| d^3r', \quad (1)$$

where Z_A is the charge of nucleus A located at R_A, $\rho(r\prime)$ is the electronic density function of the molecule, and $r\prime$ is the dummy integration variable.

The MEP is related to the electronic density and is a very useful descriptor in understanding sites of electrophilic attack and nucleophilic reactions as well as hydrogen bonding

Table 4. Mulliken atomic charges of the title compound

Atom	B3LYP/6-31G(d, p)	B3LYP/6-311G(d, p)
S1	0.221	0.228
N1	−0.504	−0.350
N2	−0.409	−0.308
H2	0.272	0.228
N3	−0.454	−0.353
H3	0.261	0.222
C1	−0.132	−0.190
H1	0.106	0.124
C2	−0.184	−0.111
H2A	0.099	0.112
H2B	0.093	0.111
C3	−0.036	−0.285
C4	−0.166	−0.087
H4A	0.096	0.112
H4B	0.104	0.115
C5	0.116	−0.045
C6	−0.120	−0.063
H6	0.082	0.088
C7	−0.088	−0.091
H7	0.082	0.091
C8	−0.086	−0.091
H8	0.081	0.091
C9	−0.088	−0.091
H9	0.082	0.090
C10	−0.120	−0.063
H10	0.079	0.085
C11	−0.304	−0.186
H11A	0.105	0.106
H11B	0.099	0.096
H11C	0.107	0.108
C12	0.305	0.150
C13	−0.356	−0.332
H13	0.120	0.128
C14	0.311	0.201
C15	0.294	0.138
C16	−0.097	−0.059
H16	0.104	0.111
C17	−0.096	−0.100
H17	0.087	0.096
C18	−0.089	−0.096
H18	0.082	0.091
C19	−0.090	−0.099
H19	0.086	0.094
C20	−0.131	−0.106
H20	0.076	0.088

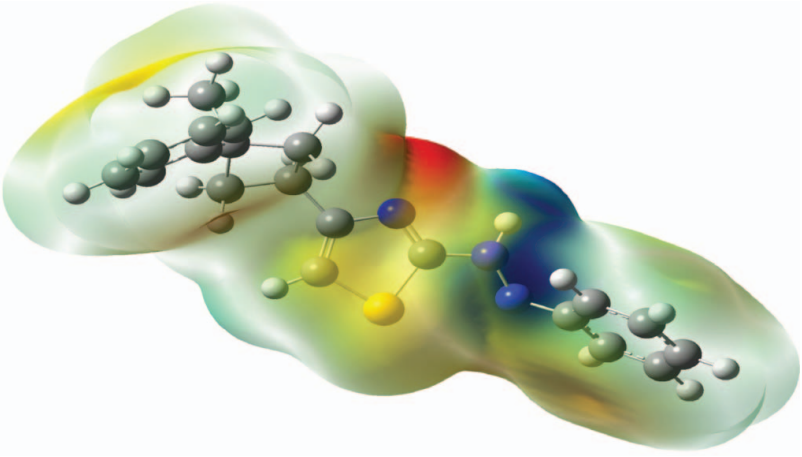

Figure 5. Molecular electrostatic potential (MEP) map calculated at B3LYP/6-31G(d, p) level.

interactions [37–39]. The electrostatic potential $V(r)$ is also well suited for analyzing processes based on the "recognition" of one molecule by another, such as in drug–receptor and enzyme–substrate interactions, because it is through their potentials that the two species first "see" each other [40,41]. Being a real physical property, $V(r)$ can be determined experimentally by diffraction or computational methods [42].

MEP was calculated using the RB3LYP/6-31G(d,p) method. The red regions and blue regions of the MEP represent negative and positive charges, respectively. As can be seen in Fig. 5, this molecule has one possible site of electrophilic attack. The negative region is localized on the unprotonated nitrogen atom of the thiazole ring, N1, with a minimum value of −0.041 a.u. The positive regions are mainly over the other nitrogen atoms. The positive $V(r)$ values are 0.044 a.u. for N2 and 0.048 a.u. for N3. These regions predicate to be intermolecular interactions, and Fig. 5 confirms the existence of an intermolecular N−H . . . N interaction between the protonated and the unprotonated N atoms of the title compound.

4.5. Frontier Molecular Orbitals

The FMOs are important in determining properties such as molecular reactivity and the ability of a molecule to absorb light. So, FMOs are very important for optical and electric properties [43]. Energy levels of the HOMO – 2, HOMO – 1, HOMO (highest occupied molecular orbital), LUMO (lowest occupied molecular orbital), LUMO + 1, and LUMO + 2 orbitals computed at the RB3LYP/6-31G(d, p) level for the title compound and the dimer are shown in Figs. 6(a) and (b). The electron clouds of the HOMOs and HOMO – 1 orbitals are localized on the rings of thiazole and benzene connected with a hydrazine bridge. The HOMO of the monomer corresponds to both HOMO of the top molecule and HOMO – 1 of the bottom molecule of the dimer. The HOMO – 1 of the monomer corresponds to both HOMO – 2 of the second molecule and HOMO – 3 of the first molecule of the dimer. The LUMO of the monomer is similar to both LUMO of the bottom molecule and LUMO + 1 of the top molecule of the dimer. The LUMO + 1 of the monomer is similar to both LUMO + 2 of the first molecule and LUMO + 3 of the second molecule of the dimer. The HOMO

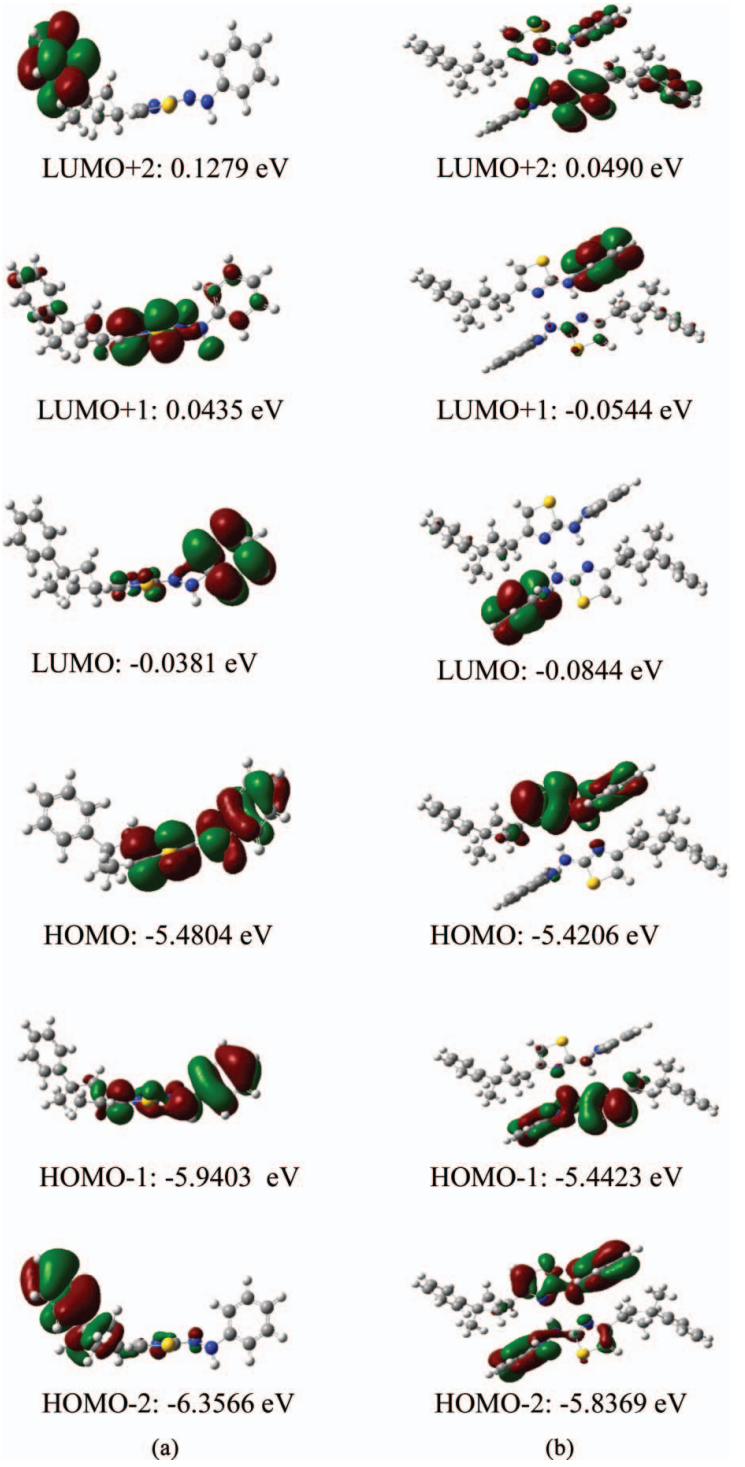

Figure 6. (a) Plots of the frontier molecular orbitals of the title compound. (b) Plots of the frontier molecular orbitals of the dimer.

Table 5. Calculated energy values and dipole moments of the title compound and the dimer

Orbital	DFT/6-31G(d, p) (monomer)	DFT/6-311G(d, p) (monomer)	DFT/6-31G(d, p) (dimer)
HOMO (a.u.)	−0.2014	−0.2098	−0.1992
LUMO (a.u.)	−0.0014	−0.0134	−0.0031
Δ (a.u.) (eV)	0.2000 (5.442)	0.1964 (5.344)	0.1961 (5.336)
Total energies (a.u.)	−1337.2	−1337.4	−2674.4
Dipole moments (D)	1.8176	1.8066	0.2151

and LUMO energies, the energy gap, total energies, and dipole moments for the monomer and the dimer have been calculated and are given in Table 5.

The HOMO–LUMO energy separation has been used as an indicator of kinetic stability of the molecule [44,45]. A large HOMO–LUMO gap implies a high kinetic stability and low chemical reactivity, because it is energetically unfavorable to add electrons to a high-lying LUMO or to extract electrons from a low-lying HOMO [45]. The HOMO – 1 and LUMO of the dimer correspond to the HOMO and LUMO of the bottom molecule of the dimer. The HOMO–LUMO energy gap for the bottom molecule is 5.358 eV. The HOMO and LUMO + 1 of the dimer correspond to the HOMO and LUMO of the top molecule of the dimer. The HOMO–LUMO energy gap for the top molecule is 5.366 eV.

In the present work, the HOMO–LUMO energy gap in the dimer form (5.336 eV) is found to be smaller than that in bottom and top molecules, which suggests that the dimer form is likely to be more reactive than the monomer form. Besides, intermolecular interactions have a significant influence in decreasing the HOMO–LUMO gaps in solids [46,47].

4.6. Vibrational Spectra

FT-IR spectra were obtained on KBr disks using a Mattson 1000 FT-IR spectrometer and are shown in Fig. 7. Harmonic vibrational frequencies of the title compound were calculated at the RB3LYP/6-31G(d, p) and RB3LYP/6-311G(d, p) levels, and the obtained frequencies were scaled by 0.9806. Using *GaussView* molecular visualization program [48], the vibrational bands assignments have been made. In order to facilitate assignment of the observed peaks, we have analyzed vibrational frequencies and compared our calculation of the title compound with the experimental results, which are shown in Table 6.

The experimental N−H asymmetric and symmetric stretchings and intra-planar bending modes were observed at 3300 cm^{-1}, 3224 cm^{-1}, and 1428 cm^{-1}, respectively. As can be easily seen, the experimental values of N−H stretching modes are smaller than the calculated frequencies, because the title compound with the hydrazine group is involved in hydrogen bonding. The experimental C=N and C=C stretch bands were observed at 1603 cm^{-1} and 1576 $cm-^{1}$, which have been calculated with 6-31G(d, p) and 6-311G(d, p) at 1588–1553 cm^{-1} and 1576–1541 $cm-^{1}$, respectively. The other calculated vibrational frequencies are presented in Table 6.

Comparing the calculated and the experimental data, we studied the relativity between the calculations and the experiments and obtained linear function formulas $y = 1.03469x$ – 51.34278 ($R^2 = 0.99807$) for B3LYP/6-31G(d, p), $y = 1.02603x$ – 43.0309 ($R^2 = 0.99795$) for B3LYP/6-311G(d, p). In these formulas, x and y are the experimental and

Table 6. Comparison of the observed and calculated vibrational spectra of the title compound

Assignments	Experimental IR with KBr (cm^{-1})	Calculated (cm^{-1}) (DFT/B3LYP) Scaled freq. (6-31G(d, p))	I(km mol^{-1})	Scaled freq. (6-311G(d, p))	*I* (km mol^{-1})
ν_{as} N−H	3300	3437	28.71	3431	30.88
ν_{s} N−H	3224	3431	8.42	3428	8.42
ν_{s} C−H (aromatic)	3179	3147	27.42	3130	25.56
ν_{s} C−H (aromatic)	3159	3142	23.12	3125	21.84
ν_{as} C−H (aromatic)	3128	3130	44.42	3113	38.26
ν_{as} C−H (aromatic)	3096	3123	11.57	3108	11.71
ν_{as} C−H (aromatic)	3082	3109	7.77	3093	6.89
ν_{as} C−H (aromatic)	3050	3107	12.70	3090	12.29
ν C−H + ν_{as} C−H_2	—	3066	31.48	3047	35.24
ν C−H + ν_{as} C−H_2 + ν_{as} C−H_3	—	3058	31.36	3039	28.63
ν_{as} C−H_2 + ν_{as} C−H_3	—	3052	13.64	—	—
ν_{as} C−H_3	3028	—	—	3028	17.34
ν_{as} C−H_3	—	3049	45.44	3026	47.91
ν_{s} C−H_2	—	3009	7.32	2994	6.82
ν_{s} C−H_2	2958	3001	32.93	2985	36.99
ν C−H	2924	2995	15.15	2982	12.20
ν_{s} C−H_3	2852	2977	25.42	2961	27.10
ν C−C (aromatic) + γ NH	—	1633	135.41	1617	146.32
ν C−C (aromatic)	—	1629	10.79	1613	11.52
ν C−C (aromatic) + γ NH	—	1621	21.80	1608	25.51
ν C=N	1603	1588	284.81	1576	275.09
ν C−C (aromatic)	1576	1553	20.96	1541	21.44
γ CH (aromatic)	—	1512	52.83	1500	38.85
γ CH (aromatic)	1546	1511	13.37	1499	16.41
γ CH (aromatic) + γ NH	1495	1502	45.67	1495	71.54
α CH_2	1443	—	—	1447	7.70
γ CH (aromatic) + γ NH	—	1443	32.57	1438	34.31
α NH	1428	1403	96.64	1406	115.91
ω CH_3	—	—	—	1384	7.22
γ CH (aromatic)	1380	1370	16.35	1363	21.51
γ CH (aromatic)	1371	1341	7.67	1329	5.59
γ CH (aromatic)+ν C=N (aromatic) + ν C−N	—	1323	18.04	1314	20.68
ν H_3CC−C (aromatic) + β CH_2	1317	1304	47.41	1295	29.55

Table 6. Comparison of the observed and calculated vibrational spectra of the title compound *(Continued)*

Assignments	Experimental IR with KBr (cm^{-1})	Calculated (cm^{-1}) (DFT/B3LYP) Scaled freq. (6-31G(d, p))	I(km mol^{-1})	Scaled freq. (6-311G(d, p))	*I* (km mol^{-1})
ν C−N + ν C−C (aromatic)	1303	—	—	1292	30.33
ν C−N (aromatic)	1264	1273	66.87	1266	75.58
ν C−N	1248	1257	106.66	1245	106.88
β CH_2 + ν C−CH_3 (aromatic)	—	1255	7.53	—	—
δ CH_2 + γ CH (aromatic)	—	—	—	1152	9.44
ν HC−C (aromatic) + γ CH (aromatic)	1176	1155	16.10	1148	10.40
ν N−N + γ CH (aromatic)	1154	1148	12.59	1142	13.02
δ CH_3 + γ CH_2 + γ CH (aromatic)	1075	1091	7.05	1087	5.54
α CH (aromatic)	—	1086	5.23	1080	6.89
α CH (aromatic)	—	1035	7.78	1030	9.54
α CH (aromatic)	1019	1033	5.79	1027	7.10
δ CH_2 + ν C−N (aromatic)	—	1016	7.94	1013	7.94
δ CH (aromatic)	889	882	8.07	885	8.87
ν S−CH	—	779	29.01	776	27.22
ω CH (aromatic)	—	765	19.06	766	20.76
ω CH (aromatic)	773	755	127.95	753	105.34
ω CH (aromatic) + ν C−S	—	747	65.09	742	82.24
γ CH (aromatic)	752	706	26.69	—	—
ω CH (aromatic) + γ CH (aromatic)	—	703	22.47	704	43.02
ω CH (aromatic) + γ CH (aromatic)	717	—	—	702	28.01
ω CH (aromatic)	—	694	8.89	695	22.37
θ (aromatic)	—	679	13.97	678	15.90
ν C−S	—	655	41.16	652	14.63
ν C−S	692	641	120.05	637	137.84
α NH	639	594	33.70	585	30.91
ω CH (aromatic)	549	546	10.72	545	16.36
ω CH (aromatic)	519	514	16.51	512	17.51
ω CH (aromatic)	496	—	—	509	8.35

Vibrational modes: ν, stretching; β, bending; α, scissoring; γ, rocking; ω, wagging; δ, twisting; θ, ring breathing; s, symmetric; as, asymmetric.

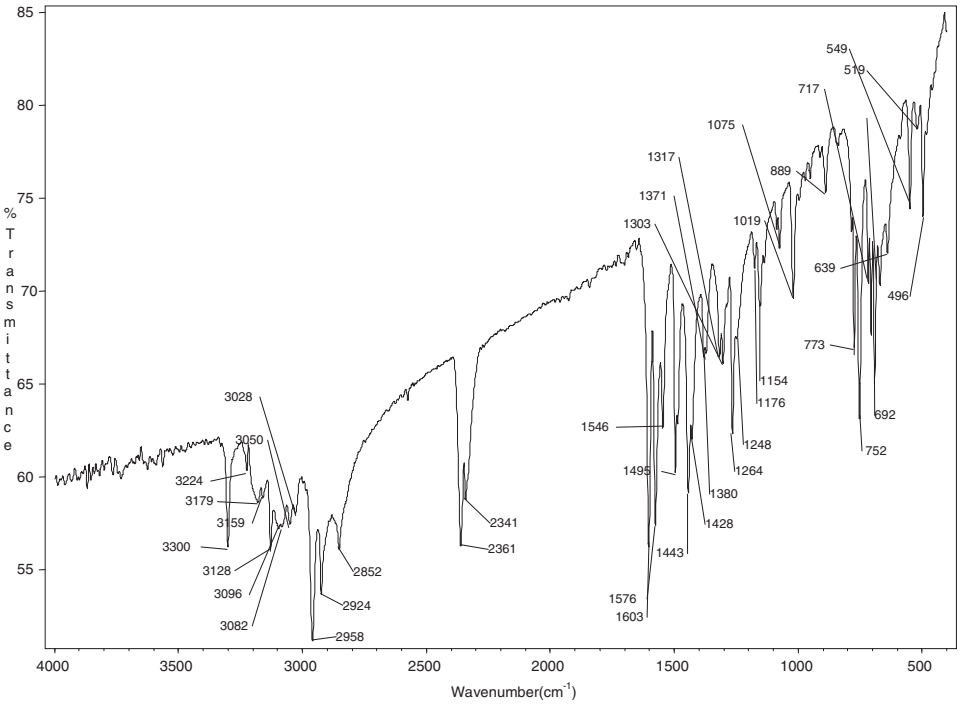

Figure 7. FT-IR spectrum of the title compound.

calculated frequencies, respectively. It can be observed from these values that the results of the RB3LYP/6-31G(d, p) method has shown a better fit to the experimental ones than the RB3LYP/6-311G(d, p) method in evaluating vibrational frequencies.

4.7. Thermodynamic Properties

On the basis of vibrational analysis at the RB3LYP/6-31G(d, p) level, the standard statistical thermodynamic functions, viz., standard heat capacity ($C^0_{p,m}$), standard entropy (S^0_m), and standard enthalpy (H^0_m), for the title compound were obtained from the theoretical frequencies and are listed in Table 7.

From Table 7, we can observe that the standard heat capacities, entropies, and enthalpies are increasing with temperatures ranging from 100 K to 1000 K due to the fact that the vibrational intensities of molecules increase with temperature. The correlation equations between these thermodynamic properties and temperature T are as follows:

$$C^0_{p,m} = -3.88416 + 0.34205T - 1.40204x10^{-4}T^2 \quad (R^2 = 0.99901) \tag{2}$$

$$S^0_m = 67.69779 + 0.32838T - 6.16918x10^{-5}T^2 \quad (R^2 = 0.99997) \tag{3}$$

$$H^0_m = -3.46405 + 0.03311T - 9.48337x10^{-5}T^2 \quad (R^2 = 0.99944). \tag{4}$$

These thermodynamic properties are needed in the detailed modeling of reaction mechanisms [49]. As we have no corresponding experimental results, we are not able to make any comparison with these results. But these data are expected to be useful for future research.

Table 7. Thermodynamic properties of the title compound at different temperatures at the B3LYP/6–31G(d, p) level

T (K)	$C^0_{p,m}$ (cal.mol^{-1}.K^{-1})	S^0_m (cal.mol^{-1}.K^{-1})	H^0_m (kcal.mol^{-1})
100.00	32.082	100.429	2.249
200.00	56.309	131.220	6.830
298.15	83.702	159.547	13.882
300.00	84.225	160.078	14.041
400.00	111.166	188.646	24.036
500.00	133.989	216.433	36.531
600.00	152.420	242.915	51.084
700.00	167.282	267.873	67.294
800.00	179.444	291.295	84.848
900.00	189.560	313.267	103.512
1000.00	198.080	333.901	123.104

4.8. Electronic Absorption Spectra

The UV-Visible (UV-Vis) absorption spectra of the title compound were recorded in a $CHCl_3$ solution. The title compound exhibits absorption peaks in the UV-Visible region. The absorption peaks are observed at 258, 242 nm for the title compound.

It is known that photon energy E is given by:

$$\mathrm{E} = \mathrm{hc}/\lambda, \tag{5}$$

where h is the Planck's constant, c is the light velocity in vacuum, and λ is the wavelength of light. For molecular maximum absorption spectrum, E can be replaced with molecular orbital energy level difference (ΔE); thus, the Equation (5) changes to [50]:

$$\Delta\mathrm{E} = \mathrm{hc}/\lambda. \tag{6}$$

Based on the photoabsorption theory, the FMOs of the title compound and the dimer have been investigated using the RB3LYP/6-31G(d, p) calculations. Three-dimensional plots of FMOs and the corresponding energy levels of the title compound and the dimer are shown in Figs 6(a) and (b), respectively. Thus, the energy level difference (ΔE) can be obtained from a two-level electron interaction according to the principle that when an electron drops from a higher level to a lower one, there is emission of a packet(s) of electromagnetic radiation. Thus, electronic transfer (ET) peaks can be determined according to Equation (6), which correspond to the experimental UV-Vis absorption peak [50]. The theoretically ET peaks for the compound determined by the RB3LYP/6-31G(d, p) and RB3LYP/6-311G(d, p) basis sets are at 228, 225 and 232, 226 nm, which correspond to the UV-Vis spectral absorption peaks, and the corresponding electronic transfers happened between HOMO and LUMO and between HOMO and LUMO + 1, respectively. The smaller theoretical absorption wavelengths of the compound have slight blue shifts compared with the corresponding experimental ones.

5. Conclusions

In this work, the compound N-[4-(3-Methyl-3-phenyl-cyclobutyl)-thiazol-2-yl]-N'-phenyl hydrazine has been characterized by elemental analysis, ^{1}H-NMR, ^{13}C-NMR, X-ray

analysis, FT-IR, and UV-Vis techniques. The X-ray structure is found to be very slightly different from its optimized counterparts, and the crystal structure is stabilized by a N—H... N-type hydrogen bond between the protonated and the unprotonated N atoms and by C—H... π interactions. The DFT RB3LYP/6-31G(d, p) and RB3LYP/6-311G(d, p) levels calculations were performed to further study the molecular structure, vibrational spectra, and electronic absorption spectra of the title compound. The results show that the optimized bond lengths are slightly longer than the experimental values, and the optimized bond angles are some different from the experimental ones. Vibrational assignments of the compound were ascribed to their structural vibrations, which show that the theoretical harmonic frequencies are in generally good agreement with their observed spectral features. The energy gap value of the title compound is between 5.336 eV and 5.442 eV. This result indicates that the title structure is quite stable. The correlations between the thermodynamic properties $C^0_{p,m}$, S^0_m, H^0_m, and temperature T were also obtained. These values can be used to calculate the other thermodynamic energies according to relationships of thermodynamic functions and to estimate directions of chemical reactions. As a result, all of these calculations will provide helpful information for further studies on the title compound.

Acknowledgment

The authors wish to acknowledge the Faculty of Arts and Sciences, Ondokuz Mayis University, Turkey, for the use of the STOE IPDS-II diffractometer (purchased under grant F.279 of the University Research Fund).

References

[1] Blair, I. A., Mansilla, T. R., Brodie, M. J., Clare, R. A., Dollery, C. T., Timbrell, J. A., & Beever, I. A. (1985). *Hum. Toxicol.*, *4*, 195.
[2] Timbrell, J. A., & Harland, S. J. (1979). *Clin. Pharmacol. Ther.*, *26*, 81.
[3] Jenner, A. M., & Timbrell, J. A. (1994). *Arch. Toxicol.*, *68*, 348.
[4] Moloney, S. J., & Prough, R. A. (1983). *Rev. Biochem. Toxicol.*, *5*, 313.
[5] Balo, J. (1979). *Adv. Cancer Res.*, *30*, 151.
[6] Clarke, D. A., Leeder, L. G., Foulds, E. I., & Trout, D. L. (1970). *Biochem. Pharmacol.*, *19*, 1743.
[7] Waterfield, C. J., Delaney, J., Kerai, M. D. J., & Timbrell, J.A. (1997). *Toxicol. In Vitro.*, *11*, 217.
[8] Bosan, W. S., Shank, R. C., MacEwen, J. D., Gaworski, C. L., & Newberne, P. M. (1987). *Carcinogenesis*, *8*, 439.
[9] Roberge, A., Gosslin, C., & Charbonneau, R. (1971). *Biochem. Pharmacol.*, *20*, 2231.
[10] Waterfield, C. J., Asker, D. S., & Timbrell, J. A. (1997). *Chem. Biol. Int.*, *107*, 157.
[11] Rothgery, E. F. (2005). *Kirk-Othmer Encyclopedia of Chemical Technology*, 5th edition, Wiley: Hoboken, NJ.
[12] Schmidt, E. W. (2001). *Hydrazine and Its Derivatives: Preparation, Properties, Applications*, 2nd edition, Wiley: Hoboken, NJ.
[13] Hadjipavlou-Litina, J. D., Geronikaki, A., & Forsch, A. (1996). *Drug Res.*, *46*, 805.
[14] Holla, B. S., Malini, K. V., Rao, B. S., Sarojini, B. K., & Kunari, N. S. (2003). *Eur. J. Med. Chem.*, *38*, 313.
[15] Allan, R. D., Hanrahan, J. R., Hambley, T. W., Johnston, G. A., Mewett, K. N., & Mitrovic, A. D. (1990). *J. Med. Chem. 33*, 2905.
[16] Lanthorn, T. H., Hood, W. F., Watson, G. B., Compton, R. P., Rader, R. K., Gaoni, Y., & Moanhan, J. B. (1990). *Eur. J. Pharmacol. 182*, 397.
[17] Gaoni, Y., Chapman, A. G., Parvez, N., Pook, P. C. K., Jane, D. E., & Watkins, J. C. (1994). *J. Med. Chem.*, *3*, 4288.

[18] Proft, F. D., & Geerlings, P. (2001). *Chem. Rev.*, *101*, 1451.
[19] Fitzgerald, G., & Andzelm, J. (1991). *J. Phys. Chem.*, *95*, 10531.
[20] Ziegler, T. (1991). *Pure Appl. Chem.*, *63*, 873.
[21] Andzelm, J., & Wimmer, E. (1992). *J. Chem. Phys.*, *96*, 1280.
[22] Scuseria, G. E. (1992). *J. Chem. Phys.*, *97*, 7528.
[23] Dickson, R. M., & Becke, A. D. (1993). *J. Chem. Phys.*, *99*, 3898.
[24] Johnson, B. G., Gill, P. M. W., & Pople, J. A. (1993). *J. Chem. Phys.*, *98*, 5612.
[25] Oliphant, N., & Bartlett, R. J. (1994). *J. Chem. Phys.*, *100*, 6550.
[26] Akhmedov, M. A., Sardarov, I. K., Akhmedov, I. M., Kostikov, R. R., Kisin, A. V., & Babaev, N. M. (1991). *Zh. Org. Khim. (USSR)*, *27*, 1434.
[27] Sheldrick, G. M. (1997). *SHELXS-97 and SHELXL-97*, University of Gottingen: Gottingen.
[28] Frisch, M. J., Trucks, G. W., Schlegel, H. B., Scuseria, G. E., Robb, M. A., Cheeseman, J. R., Montgomery, Jr., J. A., Vreven, T., Kudin, K. N., Burant, J. C., Millam, J. M., Iyengar, S. S., Tomasi, J., Barone, V., Mennucci, B., Cossi, M., Scalmani, G., Rega, N., Petersson, G. A., Nakatsuji, H., Hada, M., Ehara, M., Toyota, K., Fukuda, R., Hasegawa, J., Ishida, M., Nakajima, T., Honda, Y., Kitao, O., Nakai, H., Klene, M., Li, X., Knox, J. E., Hratchian, H. P., Cross, J. B., Bakken, V., Adamo, C., Jaramillo, J., Gomperts, R., Stratmann, R. E., Yazyev, O., Austin, A. J., Cammi, R., Pomelli, C., Ochterski, J. W., Ayala, P. Y., Morokuma, K., Voth, G. A., Salvador, P., Dannenberg, J. J., Zakrzewski, V. G., Dapprich, S., Daniels, A. D., Strain, M. C., Farkas, O., Malick, D. K., Rabuck, A. D., Raghavachari, K., Foresman, J. B., Ortiz, J. V., Cui, Q., Baboul, A. G., Clifford, S., Cioslowski, J., Stefanov, B. B., Liu, G., Liashenko, A., Piskorz, P., Komaromi, I., Martin, R. L., Fox, D. J., Keith, T., Al-Laham, M. A., Peng, C. Y., Nanayakkara, A., Challacombe, M., Gill, P. M. W., Johnson, B., Chen, W., Wong, M. W., Gonzalez, C., & Pople, J. A. (2004). *Gaussian 03. Revision E.01*. Gaussian, Inc.: Wallingford, CT.
[29] Farrugia, L. J. (1997). *J. Appl. Crystallogr.*, *30*, 565.
[30] Allen, F. H. (1984). *Acta Cryst.*, *B40*, 64.
[31] Swenson, D. C., Yamamoto, M., & Burton, D. J. (1997). *Acta Crystallogr.*, *C53*, 1445.
[32] Özdemir, N., Dinçer, M., Çukurovali, A., & Büyükgüngör, O. (2009). *J. Mol. Model.*, *15*(2), 1435.
[33] Dinçer, M., Özdemir, N., Yılmaz, İ., Çukurovali, A., & Büyükgüngör, O. (2004). *Acta Crystallogr.*, *C60*, o674.
[34] Bernstein, J., Davis, R. E., Shimoni, L., & Chang, N. L. (1995). *Angew. Chem. Int. Ed. Engl.*, *34*, 1555.
[35] Weiqun, Z., Baolong, L., Yang, C., Yong, Z., & Xujie, L. L. Y. (2005). *J. Mol. Struct. Theochem.*, *715*, 117.
[36] Politzer, P., & Murray, J. S. (2002). *Theor. Chem. Acc.*, *108*, 134.
[37] Scrocco, E., & Tomasi, J. (1978). *Adv. Quant. Chem.*, *11*, 115.
[38] Luque, F. J., Lopez, J. M., & Orozco, M. (2000). *Theor. Chem. Acc.*, *103*, 343.
[39] Okulik, N., & Jubert, A. H. (2005). *Internet Electron. J. Mol. Des.*, *4*, 17.
[40] Politzer, P., Laurence, P. R., Jayasuriya, K., & McKinney, J. (1985). *Environ. Health. Perspect.*, *61*, 191.
[41] Scrocco, E., & Tomasi, J. (1973). *Top. Curr. Chem.*, *7*, 95.
[42] Politzer, P., & Truhlar, D. G. (1981). *Chemical Applications of Atomic and Molecular Electrostatic Potentials*, Plenum Press: New York.
[43] Fleming, I. (1976). *Frontier Orbitals and Organic Chemical Reactions*, Wiley: London.
[44] Kim, K. H., Han, Y. K., & Jung, J. (2005). *Theor. Chem. Acc.*, *113*, 233.
[45] Aihara, J. (1999). *J. Phys. Chem. A*, *103*, 7487.
[46] Zheng, S.-L., Zhang, J.-P., Chen, X.-M., Huang, Z.-L., Lin, Z.-Y., & Wong, W.-T. (2003). *Chem. Eur. J.*, *9*, 3888.
[47] Zheng, S.-L., Zhang, J.-P., Wong, W.-T., & Chen, X.-M. (2003). *J. Am. Chem. Soc.*, *125*, 6882.
[48] Frisch, A., Dennington, R. I. I., Keith, T., Millam, J., Neilsen, A. B., Holder, A. J., & Hiscocks, J. (2007). *GaussView reference, Version 4.0*, Gaussian, Inc.: Pittsburg, PA.
[49] Xu, C.-X., & Chen, L.-Z. (2010). *Struct. Chem*, *21*, 9.
[50] Sun, Y.-X., Wei, W.-X., Hao, Q.-L., Lu, L.-D., & Wang, X. (2009). *Spectrochim. Acta*, *A73*, 772.